Available online at www.sciencedirect.com
SCIENCE DIRECT
Journal of Molecular Catalysis A: Chemical 255 (2006) 69–73
JOURNAL OF MOLECULAR CATALYSIS A: CHEMICAL
www.elsevier.com/locate/molcata

Physical property and chemical composition distribution of ethylene–hexene copolymer produced by metallocene/Ziegler–Natta hybrid catalyst

Hai Woong Park [a], Jin Suk Chung [b], Sung-Hyeon Baeck [c], In Kyu Song [a,*]

[a] *School of Chemical and Biological Engineering, Institute of Chemical Processes, Seoul National University, Shinlim-dong, Kwanak-ku, Seoul 151-744, South Korea*
[b] *School of Chemical Engineering and Bioengineering, University of Ulsan, Ulsan 680-749, South Korea*
[c] *Department of Chemical Engineering, Inha University, Incheon 402-751, South Korea*

Received 5 January 2006; received in revised form 3 April 2006; accepted 3 April 2006
Available online 5 May 2006

Abstract

Silica–magnesium bisupport (SMB) was prepared by a sol–gel method for use as a support for metallocene and metallocene/Ziegler–Natta hybrid catalysts. SMB was treated with methylaluminoxane (MAO) prior to catalyst immobilization. The supported heterogeneous catalysts were applied to the ethylene copolymerization with 1-hexene. The h-copolymer (ethylene–hexene copolymer produced by metallocene/Ziegler–Natta hybrid catalyst) showed two melting points and broad molecular weight distribution. The differences in physical properties between h-copolymer and m-copolymer (ethylene–hexene copolymer produced by metallocene catalyst) could be explained by the differences in chemical composition and side chain distributions of the produced copolymers.

Keywords: Ethylene–hexene copolymer; Metallocene; Ziegler–Natta; Hybrid catalyst; Chemical composition distribution; Stepwise crystallization

1. Introduction

Linear low-density polyethylene (LLDPE), typically obtained by copolymerization of ethylene with various alpha olefins such as 1-butene, 1-hexene, and 1-octene, is an important chemical product in the petrochemical industry. LLDPE has similar properties to LDPE, but has better strength properties in film applications [1]. The mechanical, optical, and rheological properties of LLDPE are strongly affected by chemical composition distribution (CCD) (also referred to as side chain distribution), molecular weight (M_w), and molecular weight distribution (MWD) [2,3]. Although LLDPE produced by metallocene catalyst shows excellent mechanical and optical properties due to narrow MWD and CCD, it also has limitation in polymer processing due to narrow MWD [4]. Metallocene catalyst systems are basically homogeneous systems. Therefore, major studies on the metallocene catalysts have been done to heterogenize in order for use in the existing commercial gas or slurry phase processes [5,6]. On the other hand, LLDPE produced by Ziegler–Natta catalyst shows broad MWD and CCD due to the irregularity of catalytic active sites.

In order to take advantage of both metallocenes and Ziegler–Natta catalysts, the blending of polyethylenes produced in two different reactors containing different metallocene catalysts or the combination of metallocene and Ziegler–Natta catalysts in a single reactor has been reported [7–11]. However, the physical blending of two different polyethylenes might be limited in the polymer processing because they could not be mixed on a molecular level. Another report to hybridize metallocene catalyst with Ziegler–Natta catalyst is to use a silica–magnesium bisupport (SMB). It was prepared by a sol–gel method in order to immobilize both metallocene and Ziegler–Natta catalysts on the same support [12]. It was reported that both silica and magnesium chloride species were dispersed on the surface and inside of SMB, and therefore, SMB served as an excellent support for the preparation of metallocene/Ziegler–Natta hybrid catalyst. HDPE [13] and LLDPE [14,15] produced by metallocene/Ziegler–Natta hybrid catalysts showed broad and

* Corresponding author. Tel.: +82 2 880 9227; fax: +82 2 888 7295.
E-mail address: inksong@snu.ac.kr (I.K. Song).

1381-1169/$ – see front matter © 2006 Elsevier B.V. All rights reserved.
doi:10.1016/j.molcata.2006.04.004

bimodal molecular weight distributions, leading to improved processability of the polymer [16,17].

In this work, silica–magnesium bisupport (SMB) was prepared by a sol–gel method for use as a support for metallocene and metallocene/Ziegler–Natta hybrid catalysts. The prepared catalysts were applied to the ethylene copolymerization with 1-hexene. The effects of hybridization of Ziegler–Natta catalyst with metallocene catalyst on the molecular weight (M_w), molecular weight distribution (MWD), melting temperature (T_m), and chemical composition distribution (CCD) of the produced ethylene–hexene copolymer were investigated.

2. Experimental

2.1. Materials

High purity ethylene (World Gas) and nitrogen (Daesung Gas) were further purified by sequential passage through columns containing molecular sieve 5A (Kokusan Chemical Works) and anhydrous P_2O_5 (Yakuri Chemicals). Toluene (Samjun Chemicals) and 1-hexene (Aldrich) were purified by distillation over sodium metal. $MgCl_2$ (Junsei Chemical), colloidal SiO_2 (LUDOX HS-40, Aldrich), *rac*-Et(Ind)$_2$ZrCl$_2$ (Strem), $TiCl_4$ (Aldrich), methylaluminoxane (MAO, Albermale), and triethylaluminum (TEA, Aldrich) were used without further purification.

2.2. Preparation of silica–magnesium bisupport (SMB) treated with methylaluminoxane (MAO)

Silica–magnesium bisupport (SMB) treated with methylaluminoxane (MAO) was prepared according to the similar method in a previous report [12]. $MgCl_2$ was dissolved in distilled water (100 ml), and pH of the solution was adjusted at 6.4 by adding H_2SO_4. The resulting solution was introduced into corn oil (2.5 l), and it was stirred at 2000 rpm for uniform dispersion. Colloidal silica (80 ml) was then introduced into the mixed solution of corn oil and $MgCl_2$. The agglomerated particles separated from the solution were washed seven times with *n*-heptane, and they were dried at 110 °C in a nitrogen stream to yield silica–magnesium bisupport. Silica–magnesium bisupport (SMB) (6 g) was suspended in toluene (100 ml), and then methylaluminoxane (MAO, 10 wt.% in toluene) (100 ml) was introduced into the slurry for 2 h at 0 °C. The mixture was stirred at 0, 20, 40, and 60 °C for 30 min each, and then finally at 80 °C for 2 h. SMB treated with MAO was washed seven times with toluene and dried under vacuum.

2.3. Preparation of supported catalyst

MAO-treated SMB (MAO/SMB, 5 g) was suspended in toluene (100 ml), and it was reacted with $TiCl_4$ (5 ml) or *rac*-Et(Ind)$_2$ZrCl$_2$ (0.5 g) at 50 °C for 2 h. The resulting slurry was washed seven times with toluene (100 ml) and dried under vacuum to obtain $TiCl_4$/MAO/SMB or *rac*-Et(Ind)$_2$ZrCl$_2$/MAO/SMB. $TiCl_4$/MAO/SMB was further reacted with *rac*-Et(Ind)$_2$ZrCl$_2$ (0.5 g) dissolved in toluene (20 ml), and the resulting slurry was washed seven times with toluene (100 ml) and dried under vacuum to yield *rac*-Et(Ind)$_2$ZrCl$_2$/TiCl$_4$/MAO/SMB.

2.4. Copolymerization of ethylene with 1-hexene

Toluene (500 ml), supported catalyst (0.04 g), 1-hexene (5 ml), and prescribed amount of cocatalyst (triethylaluminum (TEA) and/or methylaluminoxane (MAO)) were introduced into a glass reactor (1000 ml) equipped with a magnetic stirrer under the nitrogen flow. Cocatalyst ratio with respect to transition metal was fixed at Al/Ti = 300 (TEA) and Al/Zr = 3000 (MAO). After nitrogen in the reactor was evacuated, the temperature of reactor was maintained at 55 °C. Copolymerization was initiated by introducing ethylene at a constant pressure of 1.3 atm. After 40 min reaction, the polymerization was stopped by adding methanol.

2.5. Characterization of supported catalyst and ethylene–hexene copolymer

Elemental analysis of supported catalyst was done by ICP-AES (ICPs-10001V). Melting point of ethylene–hexene copolymer was determined by DSC (differential scanning calorimeter, TA 2010) with a heating rate of 10 °C/min. Molecular weight (M_w) and molecular weight distribution (MWD) were determined by GPC (gel permeation chromatography, SSC-7100) at 135 °C using *o*-dichlorobenzene as a solvent. The GPC column was calibrated with standard polystyrene. 1-Hexene content and triad sequence in ethylene–hexene copolymer were analyzed by 125 MHz ^{13}C NMR (nuclear magnetic resonance spectrometer, Avance 500) at 125 °C on the basis of Randall method [18].

A stepwise annealing procedure was conducted to analyze the chemical composition distribution (CCD) of ethylene–hexene copolymer [19–21]. As shown in Fig. 1, temperature was increased up to 160 °C with a rate of 10 °C/min and maintained for 2 h for complete melting. The melted polymer was slowly cooled at 137, 130, 123, 116, 109, 102, 95, 88, 81, and 74 °C for 2 h, respectively, and was finally cooled to 30 °C with a rate of 10 °C/min. And then the chemical composition distribution of ethylene–hexene copolymer was determined using

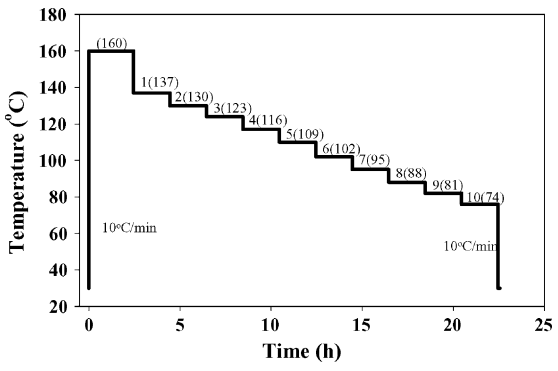

Fig. 1. Stepwise annealing procedure for chemical composition distribution analysis of ethylene–hexene copolymer.

Table 1
Elemental analyses of metallocene and metallocene/Ziegler–Natta hybrid catalysts supported on MAO-treated SMB (silica–magnesium bisupport)

Catalyst	Al (wt.%)	Ti (wt.%)	Zr (wt.%)
rac-Et(Ind)$_2$ZrCl$_2$/MAO/SMB	14.68	–	1.70
rac-Et(Ind)$_2$ZrCl$_2$/TiCl$_4$/MAO/SMB	10.67	4.86	0.55

DSC with a heating rate of 10 °C/min. Lamella thickness of fractionated ethylene–hexene copolymer was calculated by the Thomson–Gibbs equation [22].

3. Results and discussion

3.1. Elemental analyses of supported catalysts on MAO-treated SMB

Table 1 shows the ICP-AES elemental analyses of catalysts supported on MAO-treated SMB. It was observed that 0.55 wt.% of zirconium and 4.86 wt.% of titanium were immobilized on the *rac*-Et(Ind)$_2$ZrCl$_2$/TiCl$_4$/MAO/SMB catalyst, while 1.70 wt.% of zirconium was impregnated on the *rac*-Et(Ind)$_2$ZrCl$_2$/MAO/SMB catalyst. Aluminum contents originated from MAO were 10.67 and 14.68 wt.% in each catalyst, respectively. It is believed that MAO-treated SMB served as a suitable support for the immobilization of *rac*-Et(Ind)$_2$ZrCl$_2$/TiCl$_4$ and *rac*-Et(Ind)$_2$ZrCl$_2$.

3.2. Catalytic activities and physical properties of ethylene–hexene copolymer

Table 2 shows the catalytic activities of supported catalysts and the physical properties of prepared ethylene–hexene copolymer. As also shown in Fig. 2, the catalytic activity of *rac*-Et(Ind)$_2$ZrCl$_2$/MAO/SMB was superior to that of *rac*-Et(Ind)$_2$ZrCl$_2$/TiCl$_4$/MAO/SMB. It is believed that the different content of zirconium on each catalyst is mainly responsible for the difference in catalytic activity because the catalytic activity of metallocene was much higher than that of Ziegler–Natta catalyst on SMB [12]. Catalytic activity of *rac*-Et(Ind)$_2$ZrCl$_2$/MAO/SMB was not maintained constant but decreased steadily with time on stream. This trend is well consistent with that observed in the typical homogenous metallocene catalyst. On the other hand, the activity profile of *rac*-Et(Ind)$_2$ZrCl$_2$/TiCl$_4$/MAO/SMB was not changed significantly with time on stream.

Molecular weight (M_w) of ethylene–hexene copolymer produced by *rac*-Et(Ind)$_2$ZrCl$_2$/MAO/SMB and *rac*-Et(Ind)$_2$ZrCl$_2$/TiCl$_4$/MAO/SMB was 0.1×10^6 and 0.25×10^6 g/mol, respectively. M_w of h-copolymer (produced by hybrid catalyst) was similar to that of m-copolymer (produced by metallocene catalyst). The molecular weight distribution (MWD) of h-copolymer was broadened to 30.6 compared to 2.6 of m-copolymer because two different kinds of active sites in the hybrid catalyst produced copolymers with different molecular weight range. The 1-hexene content of m-copolymer was larger than that of h-copolymer (Table 2). As we mentioned above in the explanation for the activity difference, the different content of zirconium on each catalyst could lead to the difference in comonomer content. It is known that the comonomer incorporability of metallocene active site is superior to that of Ziegler–Natta active site.

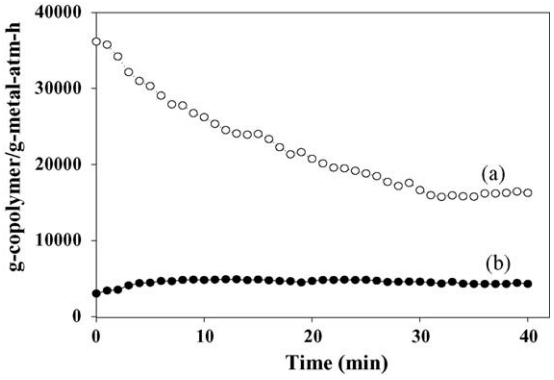

Fig. 2. Activity profiles of supported catalysts in the ethylene copolymerization with 1-hexene: (a) *rac*-Et(Ind)$_2$ZrCl$_2$/MAO/SMB (Al/Zr = 3000) and (b) *rac*-Et(Ind)$_2$ZrCl$_2$/TiCl$_4$/MAO/SMB (Al/Zr = 3000, Al/Ti = 300).

The melting temperature (T_m) of m-copolymer was found to be 122.6 °C, as shown in Fig. 3. On the other hand, h-copolymer showed two melting peaks at 115.6 and 126.5 °C resulting from two kinds of active site, metallocene and Ziegler–Natta. It is interesting to observe that the melting peak of h-copolymer caused by metallocene active sites over *rac*-Et(Ind)$_2$ZrCl$_2$/TiCl$_4$/MAO/SMB has shifted to the lower temperature (122.6 → 115.6 °C) in spite that h-copolymer has lower 1-hexene content and higher molecular weight than m-copolymer.

The chemical composition distribution of each comonomer, an average sequence length ($\bar{n}$), and triad sequences were analyzed with ^{13}C NMR. As shown in Fig. 4, nine peaks (A1–A5 and B1–B4) detected by ^{13}C NMR were distributed in the range of 10–40 ppm. A butyl branch (B1–B4) was observed in both m-copolymer and h-copolymer as a result of successful copolymerization of ethylene with 1-hexene. The triad sequences of m-copolymer and h-copolymer were analyzed on the basis of

Table 2
Catalytic activities of supported catalysts and physical properties of prepared ethylene–hexene copolymer

Catalyst	Cocatalyst ratio	Catalytic activity (g-copolymer/g-metal atm h)	M_w ($\times 10^{-6}$)	MWD	T_m (°C)	1-Hexene (mol%)
rac-Et(Ind)$_2$ZrCl$_2$/MAO/SMB	Al/Zr = 3000	25500	0.1	2.6	122.6	5.6
rac-Et(Ind)$_2$ZrCl$_2$/TiCl$_4$/MAO/SMB	Al/Zr = 3000, Al/Ti = 300	5300	0.25	30.6	115.6, 126.5	3.0

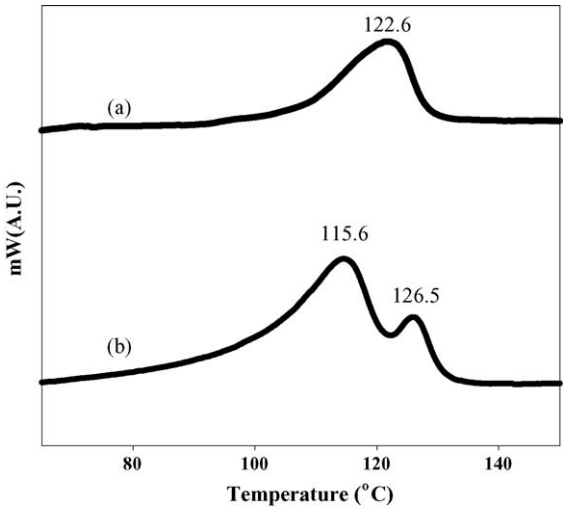

Fig. 3. DSC profiles of (a) m-copolymer and (b) h-copolymer.

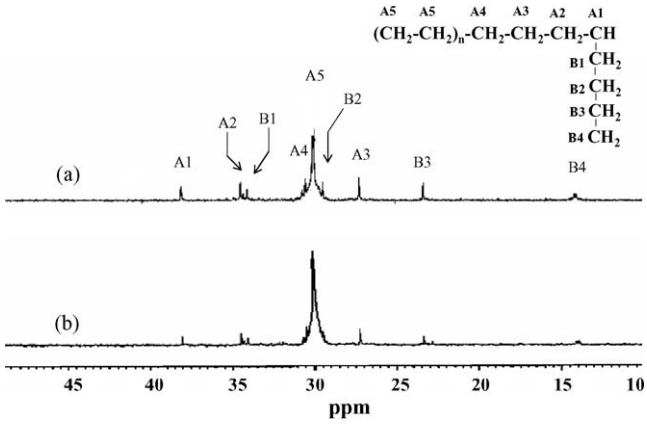

Fig. 4. ^{13}C NMR peaks of (a) m-copolymer and (b) h-copolymer.

Randall method as listed in Table 3. Neither [HHH] nor [HEH] was observed in both m-copolymer and h-copolymer. There was no great difference in [EHH] sequence between m-copolymer and h-copolymer, indicating that h-copolymer contained similar amount of blocky 1-hexene sequence compared to m-copolymer although the amount of 1-hexene content in the m-copolymer was larger than that in the h-copolymer. However [EHE] and [HEE] sequences in the h-copolymer were much lower than those in the m-copolymer. It was also observed that the average sequence length ($\tilde{n}$) of the h-copolymer was longer than that of the m-copolymer, even though less amount of 1-hexene was incorporated in the h-copolymer.

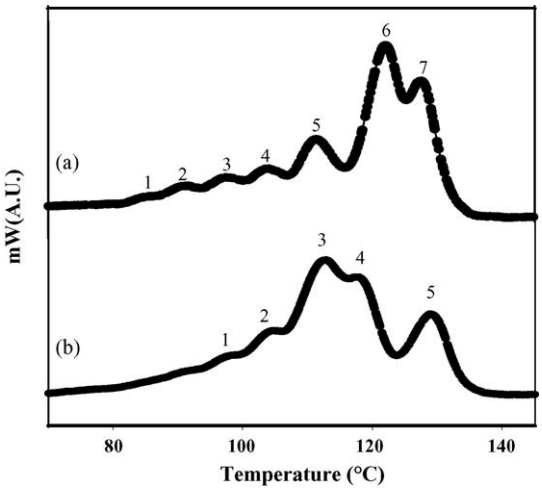

Fig. 5. Chemical composition distribution evaluated by stepwise annealing procedure: (a) m-copolymer and (b) h-copolymer.

3.3. Chemical composition distribution of the produced copolymer evaluated by a stepwise crystallization

As mentioned previously, we have observed that the melting peak of h-copolymer caused by metallocene active sites over hybrid catalyst has shifted to the lower temperature. To investigate this result, the chemical composition distribution (CCD) of the produced copolymer was analyzed by a stepwise crystallization. As shown in Fig. 5, seven peaks in m-copolymer and five peaks in h-copolymer were observed by stepwise crystallization with DSC analysis. Table 4 summarizes the lamella thickness of fractionated copolymer and its distribution determined on the basis of the Thomson–Gibbs equation [22]. Approximately 5 wt.% of lamellas in the m-copolymer was observed in the range of 35–41 Å thickness, but we could not observe them in the h-copolymer. In other words, lamellas in low temperature range (<95 °C) were not observed in the h-copolymer. Over 60 wt.% of lamella in the m-copolymer was distributed in the range over 100 Å. On the other hand, 21 wt.% of lamella over 100 Å and 58% of lamella in the range of 70–87 Å were observed in the h-copolymer. These results indicate that the hybrid catalyst produced the narrower lamella size distribution than the metallocene catalyst as a result of hybridization. Based on these analyses, it is believed that the melting peak caused by metallocene active sites in the h-copolymer shifted to the low temperature compared to the melting point of m-copolymer, although h-copolymer had lower 1-hexene content and higher molecular weight than m-copolymer.

Table 3
Comonomer content, average sequence length, and triad sequence in ethylene–hexene copolymer

Catalyst	Polymer	Comonomer content (mol%)		Average sequence length		Triad sequence (mol%)					
		[H]	[E]	$\tilde{n}_E$	$\tilde{n}_H$	[EHE]	[EHH]	[HHH]	[HEH]	[HEE]	[EEE]
rac-Et(Ind)$_2$ZrCl$_2$/MAO/SMB	m-Copolymer	5.6	94.4	20.5	1.2	3.60	1.99	0	0	9.20	85.20
rac-Et(Ind)$_2$ZrCl$_2$/TiCl$_4$/MAO/SMB	h-Copolymer	3.0	97.0	46.1	1.4	1.26	1.69	0	0	4.21	92.48

E: ethylene; H: 1-hexene.

Table 4
Lamella thickness and its distribution in ethylene–hexene copolymer

Catalyst	Polymer	Peak number	T_m (°C)	Lamella thickness (Å)	wt.%
rac-Et(Ind)$_2$ZrCl$_2$/MAO/SMB	m-Copolymer	1	83	35.6	0.9
		2	92	41.3	4.5
		3	98	46.5	6.1
		4	105	55.7	8.3
		5	111	67.7	17.4
		6	122	105.8	38.6
		7	128	152.1	24.2
rac-Et(Ind)$_2$ZrCl$_2$/TiCl$_4$/MAO/SMB	h-Copolymer	1	99	47.7	7.7
		2	104	54.7	12.7
		3	113	70.8	35.7
		4	118	87.4	22.9
		5	129	167.2	21.0

4. Conclusions

Metallocene and metallocene/Ziegler–Natta hybrid catalysts supported on silica–magnesium bisupport (SMB) efficiently catalyzed the ethylene copolymerization with 1-hexene. Copolymer produced by the hybrid catalyst showed two melting points and broad molecular weight distribution due to two kinds of active sites. The differences in chemical composition and side chain distributions of the produced copolymers were observed as a result of hybridization. It was found that the copolymer produced by hybrid catalyst showed the narrower lamella size distribution than that produced by metallocene catalyst.

Acknowledgement

The authors acknowledge the financial support of Taeyoung Industry Corporation for this work (Grant No. 0458-20050005).

References

[1] H.S. Cho, W.Y. Lee, Korean J. Chem. Eng. 19 (2002) 557.
[2] A.J. Müller, Z.H. Hernandez, M.L. Arnal, J. Sábchez, J. Polym. Bull. 39 (1997) 465.
[3] U. Zucchini, G. Checchin, Adv. Polym. Sci. 51 (1983) 101.
[4] A. Ahlers, W. Kaminsky, Makromol. Chem. Rapid Commun. 9 (1988) 457.
[5] M. Jezequel, V. Dufaud, M.J.R. Garcia, F.C. Hermosilla, U. Neugebauer, G.P. Niccolai, F. Lefebvre, F. Bayard, J. Corker, S. Fiddy, J. Evans, J.P. Broyer, J. Malings, J.M. Basset, J. Am. Chem. Soc. 123 (2001) 3520.
[6] J. Tian, S. Wang, Y. Feng, J. Li, S. Collins, J. Mol. Catal. A 144 (1999) 137.
[7] T.O. Ahn, S.C. Hong, J.H. Kim, D.H. Lee, J. Appl. Polym. Sci. 67 (1998) 2213.
[8] A. Razavi, US Patent 5,914,289, 1999.
[9] K. Heiland, W. Kaminsky, Macromol. Chem. 601 (1992) 601.
[10] J.D. Kim, J.B.P. Soares, J. Polym. Sci. Polym. Chem. 38 (2000) 1427.
[11] K. Czaja, M. Bialek, A. Utrata, J. Polym. Sci. Polym. Chem. 42 (2004) 2512.
[12] J.S. Chung, H.S. Cho, G.Y. Ko, W.Y. Lee, J. Mol. Catal. A 144 (1999) 61.
[13] Y.G. Ko, H.S. Cho, K.H. Choi, W.H. Lee, Korean J. Chem. Eng. 16 (1999) 562.
[14] H.S. Cho, J.S. Chung, J.H. Han, Y.G. Ko, W.Y. Lee, J. Appl. Polym. Sci. 70 (1998) 1707.
[15] H.S. Cho, D.J. Choi, W.Y. Lee, J. Appl. Polym. Sci. 78 (2000) 2318.
[16] H.S. Cho, J.S. Chung, W.Y. Lee, J. Mol. Catal. A 159 (2000) 203.
[17] H.S. Cho, K.H. Choi, D.J. Choi, W.Y. Lee, Korean J. Chem. Eng. 17 (2000) 205.
[18] E.T. Hsieh, J.C. Randall, Macromolecules 15 (1982) 1402.
[19] L. Wild, T.R. Ryle, D.C. Knobeloch, I.R. Peat, J. Polym. Sci. Polym. Chem. 20 (1982) 441.
[20] P. Starch, Polym. Int. 40 (1996) 111.
[21] K. Czaja, B. Sacher, M. Bialek, J. Therm. Anal. Catal. 67 (2002) 547.
[22] D. Hosoda, Polym. J. 20 (1988) 383.